Differential optineurin expression controls TGF beta signaling and is a key determinant for metastasis of triple negative breast cancer

Liu, S.J.; Dinther, M. van; Hagenaars, S.C.; Gu, Y.Z.; Kuipers, T.B.; Mei, H.L.; ... ; Dijke, P. ten

Received: 1 September 2022 | Revised: 6 January 2023 | Accepted: 10 February 2023

DOI: 10.1002/ijc.34483

MOLECULAR CANCER BIOLOGY

IJC INTERNATIONAL JOURNAL of CANCER

Differential optineurin expression controls TGFβ signaling and is a key determinant for metastasis of triple negative breast cancer

Sijia Liu[1,2] | Maarten van Dinther[1] | Sophie C. Hagenaars[3] | Yuanzhuo Gu[1] | Thomas B. Kuipers[4] | Hailiang Mei[4] | Maria Catalina Gomez-Puerto[1] | Wilma E. Mesker[3] | Peter ten Dijke[1]

[1]Oncode Institute and Department of Cell and Chemical Biology, Leiden University Medical Center, Leiden, The Netherlands

[2]The Second Affiliated Hospital, School of Medicine, Zhejiang University, Hangzhou, China

[3]Department of Surgery, Leiden University Medical Center, Leiden, The Netherlands

[4]Department of Biomedical Data Sciences, Leiden University Medical Center, Leiden, The Netherlands

Correspondence
Peter ten Dijke, Department of Cell and Chemical Biology, Leiden University Medical Center, Postbus 9600, 2300 RC Leiden, The Netherlands.
Email: p.ten_dijke@lumc.nl

Funding information
Cancer Genomics Centre Netherlands; ZonMw, Grant/Award Number: 09120012010061

Abstract

Triple-negative breast cancer (TNBC) is the most challenging breast cancer subtype to treat due to its aggressive characteristics and low response to the existing clinical therapies. Distant metastasis is the main cause of death of TNBC patients. Better understanding of the mechanisms underlying TNBC metastasis may lead to new strategies of early diagnosis and more efficient treatment. In our study, we uncovered that the autophagy receptor optineurin (OPTN) plays an unexpected role in TNBC metastasis. Data mining of publicly available data bases revealed that the mRNA level of *OPTN* in TNBC patients positively correlates with relapse free and distance metastasis free survival. Importantly, in vitro and in vivo models demonstrated that OPTN suppresses TNBC metastasis. Mechanistically, OPTN inhibited the pro-oncogenic transforming growth factor-β (TGFβ) signaling in TNBC cells by interacting with TGFβ type I receptor (TβRI) and promoting its ubiquitination for degradation. Consistent with our experimental findings, the clinical TNBC samples displayed a negative correlation between *OPTN* mRNA expression and TGFβ gene response signature and expression of proto-typic TGFβ target genes. Altogether, our study demonstrates that OPTN is a negative regulator for TGFβ receptor/SMAD signaling and suppresses metastasis in TNBC.

KEYWORDS
metastasis, optineurin, signal transduction, transforming growth factor-β, triple negative breast cancer, ubiquitination

Abbreviations: ANOVA, analyses of variance; BM-Luc, bone metastasis luciferase; ca, constitutively active; DMEM, Dulbecco's Minimal Eagle Medium; ECL, enhanced chemiluminescence; EGFP, enhanced green fluorescent protein; ER, estrogen receptor; FBS, fetal bovine serum; HACE1, HECT domain and ankyrin repeat containing E3 ubiquitin protein ligase 1; HER2, human EGF receptor 2; IL11, interleukin 11; LUMC, Leiden University Medical Center; MTS, 3-(4,5-dimethylthiazol-2-yl)-5-(3-carboxymethoxyphenyl)-2-(4-sulfophenyl)-2H-tetrazolium; NEM, N-ethylmaleimide; OPTN, optineurin; PAI-1, plasminogen activator inhibitor-1; PBS, phosphate buffered saline; PEI, polyethylenimine; PFA, paraformaldehyde; PR, progesterone receptor; PTHrP, parathyroid hormone related protein; RT-PCR, reverse transcriptase polymerase chain reaction; sh, short hairpin; SMAD, Sma and Mad related protein; Tg, transgenic; TGFβ, transforming growth factor-β; TNBC, triple negative breast cancer; TβR, TGFβ receptor.

What's new?

Our study revealed an unexpected role for the autophagy receptor optineurin (OPTN) in triple-negative breast cancer metastasis. Low expression levels of OPTN in triple-negative breast cancer correlated with higher metastasis incidence. Mechanistically, OPTN was found to be a negative regulator of TGF-β type I receptor stability and to inhibit TGFβ-induced protumorigenic responses in triple-negative breast cancer cells. Consistently, clinical sample analysis revealed a negative correlation between OPTN mRNA expression and TGF-β receptor signaling activity. Low OPTN expression levels may be a potential prognostic indicator to stratify triple-negative breast cancer patients that are prone to develop metastasis.

1 | INTRODUCTION

Triple-negative breast cancer (TNBC) refers to the breast cancer subtype that is deficient in estrogen receptor (ER), progesterone receptor (PR), and human epidermal growth factor receptor 2 (HER2) expression.[1] Among all breast cancer cases, TNBC is the most aggressive subtype, accounting for 20% of the total breast cancer incidence.[2] As TNBC does not respond to antihormonal therapies and has relatively low response to chemo-/radio-/immunotherapy, TNBC remains the most challenging subtype in breast cancer to treat.[3] Distant metastases are the main reason of death in breast cancer, of which bone metastasis is the most common site of advanced breast cancer with an incidence rate of approximately 80%.[4] TNBC patients with bone metastasis have a shorter survival period than other subtypes, and suffer from pathologic fractures and spinal cord compression, which severely decrease the quality of life.[5] In order to develop new treatments of TNBC, it is crucial to better understand the mechanism of metastasis and find out clinically prognostic indicators for TNBC prevention, diagnosis and therapy.

The cytokine transforming growth factor β (TGFβ) signaling plays pivotal roles during cancer progression by triggering epithelial-mesenchymal transition (EMT), migration and metastasis of cancer cells.[6,7] Moreover, it controls the tumor microenvironment (TME) by acting on TME cells such as cancer-associated fibroblasts (CAFs), endothelial cells and immune cells to facilitate cancer cell metastasis.[6,7] TGFβ is often expressed at high levels in TNBC tumors.[8,9] It can be produced by cancer cells, tumor-associated stromal cells or immune cells.[8,9] Upon TGFβ binding to and activation of the TGFβ type I and type II receptor (ie, TβRI and TβRII) complex on the cell membrane, intracellular signaling is initiated by TβRI-mediated phosphorylation of SMAD2/3 intracellular effector proteins. Thereafter phosphor-SMAD2/3 interacts with SMAD4, forming heteromeric complexes, which translocate into the nucleus and initiate transcriptional activation of target genes.[10] One of the proto-typical TGFβ/SMAD target genes is plasminogen activator inhibitor-1 (PAI-1), which is potently and directly induced in a SMAD3/SMAD4 dependent manner.[11] Three other TGFβ target genes that encode for interleukin-11 (IL11), parathyroid hormone-related protein (PTHrP) and connective tissue growth factor (CTGF) play key roles in the establishment of breast cancer micro/macro metastases in bone tissue.[12-14]

Optineurin (OPTN) is a cytosolic coiled-coil containing protein that was initially identified in individuals with inherited primary open-angle glaucoma,[15] and mutations in *OPTN* were causally linked to glaucoma, Paget disease of bone, frontotemporal dementia and amyotrophic lateral sclerosis.[16] OPTN is involved in basic cellular functions including protein trafficking, maintenance of the Golgi apparatus, as well as nuclear factor (NF)-κB pathway, antiviral, and antibacterial signaling.[17] Moreover, OPTN is an autophagy receptor, which contains an ubiquitin binding domain that mediates interaction with polyubiquitinated cargoes and functions in autophagosome formation and maturation.[17] The function of OPTN in cancer have not been widely and deeply studied; In lung cancer, the E3 ubiquitin ligase HACE1-OPTN axis was identified as an cancer-suppressor via in-vitro tumor-colony-formation assays and an in-vivo xenografted nude mouse model.[18]

In our study, we found that TNBC patients with higher *OPTN* mRNA expression level correlate with a better survival. Moreover, TNBC patients with an advanced disease and occurrence of metastasis display a lower *OPTN* mRNA expression level. Mechanistically, we elucidated that OPTN inhibits TGFβ pro-oncogenic signaling and suppresses migration and metastasis of TNBC cells. Finally, consistent with our experimental finding and analysis of TNBC clinical samples, we show that increased OPTN expression correlates with lower TGFβ gene response signature.

2 | MATERIALS AND METHODS

2.1 | Ligands and chemicals

Recombinant TGFβ3 was obtained from Dr. Andrew Hinck (University of Pittsburgh), cycloheximide, N-ethlmaleimide (NEM) were obtained from Sigma, SB-43152 was obtained from Tocris. 100 U/mL penicillin/streptomycin (Thermo Fisher Scientific; Cat. No. 15140163), Dulbecco's modified Eagle medium (DMEM; Thermo Fisher Scientific; Cat. No. 41965062), MG132 (Sigma-Aldrich; Cat. No. 474787).

2.2 | Cell lines and generation of cell lines

Human HEK293T (RRID:CVCL_0063) and TNBC cell lines MDA-MB-231 (RRID:CVCL_0062) and SK-BR-7 (RRID:CVCL_5218) were

originally obtained from American Type Culture Collection (ATCC) and cultured in Dulbecco's modified Eagles medium (DMEM) supplemented with 10% fetal bovine serum (FBS) and 100 U/mL penicillin-streptomycin (15140122; Gibco).

All cell lines were authenticated using short tandem repeat (STR) profiling within in the last 3 years. All experiments were performed with mycoplasma-free cells.

2.3 | Transfections and lentiviral infection

Cells were transfected with polyethylenimine (PEI, Sigma). All the plasmids are listed in Table S1. Lentiviruses were produced as previously described.[19] OPTN short hairpin (sh)RNAs for lentiviral infection were obtained from Sigma (MISSION shRNA library). Two shRNAs were identified and tested, the most effective shRNAs, sh1-OPTN (TRCN0000083743; Sigma) and sh2-OPTN (TRCN0000083744; Sigma) were used for experiments. MDA-MB-231 bone metastasis luciferase (BM-Luc) cells were previously described.[20] MDA-MB-231 (BM-Luc) mCherry cells were made by infecting MDA-MB-231 BM-Luc cells with PLV-mCherry lentivirus and a single colony was isolated, and thereafter expanded.[21] MDA-MB-231 (BM Luc/mCherry) cells were infected with PLV-EV, PLV-OPTN-HA, PLV-OPTN-FLAG, PLKO, sh1-OPTN or sh2-OPTN lentivirus (see for details below) to generate stable cell lines with puromycin selection.

2.4 | Western blot analysis

Cells were lysed in Laemmli buffer (0.12 M Tris-HCl pH 6.8, 4% SDS, 20% glycerol, 35 mM β-mercaptoethanol and bromophenol blue) and boiled for 5 minutes. Standard procedures were used for western blotting.[22] Primary antibodies used were listed in Table S2. Secondary antibodies were conjugated to horseradish peroxidase (Amersham Biosciences). Chemiluminescence signal was imaged using ChemiDoc MP Imaging System (Bio-Rad) with Clarity Western Enhanced Chemiluminescence (ECL) substrate (1705060; Bio-Rad). All experiments were repeated at least three times in biologically independent experiments, and representative data are shown.

2.5 | IncuCyte migration assay

Equal numbers of cells were seeded in the IncuCyte 96-well Essen ImageLock plate (Cat. No. 4379, Essen BioScience), The uniform scratch wound was generated in each well using the IncuCyte WoundMaker (Essen BioScience). Floating cells were removed by a rinse with phosphate buffered saline (PBS) and then incubated with DMEM medium supplemented with 0.5% fetal bovine serum (FBS). Cells were incubated and monitored in the IncuCyte live cell imaging system (Essen BioScience). Images were acquired every 2 hours over a 48-hour period using a 10× objective. Relative wound density was analyzed by the IncuCyte cell migration software for each well. All the experiments were repeated at least three times in biologically independent experiments, and representative results are shown.

2.6 | Zebrafish extravasation assay of human breast cancer cells

Transgenic zebrafish lines Tg (*fli1*: enhanced green fluorescent protein [EGFP]) were raised and all zebrafish experiments were conducted according to standard procedures in a licensed establishment for the breeding and use of experimental animals (LU) and subject to internal regulations and guidelines, stating that advice is taken from the animal welfare body to minimize suffering for all experimental animals housed at the facility.

Zebrafish extravasation assays were prepared as previously described.[21] Zebrafish were fixed with 4% paraformaldehyde (PFA) 5 days after injection. Imaging and quantification of the results were carried out on an inverted SP5 STED confocal microscope (Leica), At least 40 zebrafish were analyzed for each group and three representative images were taken. All the experiments were repeated at least three times, and representative results are shown.

2.7 | Breast cancer bone metastasis assay in mice xenograft model

Mice were purchased from the animal husbandry center of the Netherlands Cancer Institute. For the intracardial injection, five-weeks-old female BALB/c nude mice were anesthetized with isoflurane and single-cell suspension of MDA-MB-231 BM-Luc (300.000/100ul PBS) cells were inoculated into the left heart ventricle according to the method described by Arguello et al.[23] Ten mice were injected in each group. Bioluminescent imaging was used to verify successful injection and to monitor the outgrowth of metastasis weekly. Mice experiments were approved by the Netherlands Cancer Institute Animal Welfare Committee.

2.8 | MTS cell proliferation assay

MTS (3-(4,5-dimethylthiazol-2-yl)-5-(3-carboxymethoxyphenyl)-2-(4-sulfophenyl)-2H-tetrazolium) assay was applied to assess cell proliferation as instructed by the manufacturer (Promega, Leiden, Netherlands). Cells were seed at 1000 cells per well in 100 μL/well using 96-well culture plates. The absorbance of the samples was measured at 490 nm on a scanning multiwell spectrophotometer. The samples were tested at 1, 2, 3, 4 and 5 days after seeding. All the experiments were repeated at least three times in biologically independent experiments and representative results are shown.

2.9 | Real-time quantitative RT-PCR

Total RNA extraction was performed using the NucleoSpin RNA II kit (MACHEREY-NAGEL) according to instructions from the manufacturer. Equal amounts of RNA were retro-transcribed using RevertAid First Stand cDNA synthesis Kits (Thermo Fisher), and real-time reverse transcription-PCR experiments were performed using SYBR Green (Promega) in CFX connect Real-Time PCR detection system (Bio-Rad). All the values for target gene expression were normalized to *GAPDH*. Primers are listed in Table S3. Numerical data from triplicates are presented as the mean ± SD. The significance of differences between two independent subjects was determined using the unpaired Student's *t* test. Two-way analysis of variance (ANOVA) has been used to analysis multiple subjects. *P* value are indicated by asterisks in the figures: "ns" indicates not significant ($P > .05$), differences at $P = .05$ and lower were considered significant. $^{*}P < .05$, $^{**}P < .01$, $^{***}P < .001$ and $^{****}P < .0001$.

2.10 | Immunoblotting and immunoprecipitation assay

HEK293T cells were lysed in 1 mL TNE lysis buffer (50 mM Tris-HCl, pH 7.4, 1 mM EDTA, 150 mM NaCl, 1% NP40) with protease inhibitor cocktail for 10 minutes on ice. The lysates were centrifuged at 16×10^3g for 10 minutes at 4°C, thereafter protein concentrations were measured using the DC protein assay (Pierce) and equal amounts of proteins were used for each condition that was analyzed by immunoblotting. For the immunoprecipitation assay, equal amounts of protein were incubated with anti-FLAG agarose beads (A2220; Sigma) at 4°C for 2 hours or with different antibodies overnight and protein A/G-Sepharose (GE Healthcare Bio-Sciences AB) for 2 hours at 4°C. Beads were washed five times with TNE buffer, and thereafter boiled with sample buffer for 5 minutes and subjected to SDS-polyacrylamide gel electrophoresis (PAGE) analysis. All the experiments were repeated at least three times and representative results are shown.

2.11 | Proximity ligation assay

Cells were seeded on cover slips in a 24 well plate and cultured for 24 hours. Cells were serum starved overnight and then treated with or without 5 ng/mL TGFβ for 1 hour. Cells were fixed with 4% paraformaldehyde for 20 minutes at room temperature followed by permeabilization with 0.1% Triton X-100 for 10 minutes. Cells were blocked in blocking buffer from the kit (DUO92001-100RXN, DUO92005-100RXN) for 1 hour at 37°C and incubated in primary antibodies overnight at 4°C. On the next day, cells were washed with the wash buffer A (DUO82049) for three times and incubated with the secondary antibodies with proximity ligation assay probes (DUO92001-100RXN, DUO92005-100RXN) for 1 hour at 37°C followed by three washes with buffer A. Cells were incubated with the Duolink in situ detection reagents red (DUO92008) for 2 hours at 37°C. After three times washing with buffer B, samples were mounted with VECTASHIELD antifade mounting medium with DAPI (H-1200; Vector Laboratories) Fluorescence images were acquired with DMi8 Inverted Fluorescent Microscope (Leica). All the experiments were repeated at least three times in biologically independent experiments and representative results are shown.

2.12 | Ubiquitination and deubiquitination assays

HEK293T cells were transfected with indicated constructs and harvested 48 hours after transfection and washed twice in cold PBS with 10 mM N-ethlmaleimide (NEM) and lysed in 1% SDS-RIPA buffer (25 mM Tris-HCl, pH 7.4, 150 mM NaCl, 1% NP40, 0.5% sodium deoxycholate, and 1% SDS) supplemented with protease inhibitors and 10 mM NEM. To prevent detection of ubiquitination of coimmunoprecipitating proteins, the lysates were boiled for 5 minutes, diluted to 0.1% SDS in RIPA buffer, and incubated with anti-FLAG agarose beads for 2 hours at 4°C. After five washes with RIPA buffer, beads were boiled in loading buffer for 5 minutes and size-separated by SDS-PAGE for the ubiquitination detection. All the experiments were repeated at least three times in biologically independent experiments, and representative results are shown.

2.13 | Statistical and bioinformatic analysis

Statistical analysis was performed using Prism 8 software (GraphPad, La Jolla, USA). Numerical data from triplicates are presented as the mean ± SD, except for analysis of Zebrafish experiments where a representative result is expressed as mean ± SEM. The significance of differences between two independent subjects was determined using the unpaired Student's *t* test. Two-way analysis of variance (ANOVA) has been used to analysis multiple subjects. The Kaplan-Meier method was used to evaluate metastasis free survival of mice between two groups. P value are indicated by asterisks in the figures: $^{*}P < .05$, $^{**}P < .01$, $^{***}P < .001$ and $^{****}P < .0001$. Differences at $P = .05$ and lower were considered significant. The publicly available gene expression dataset GSE76274 derived from the R2 Genomics Analysis and Visualization Platform (R2 platform; http://r2.amc.nl) was applied for the analyses of the correlations between *OPTN* mRNA levels and TGF-β response gene signature.

3 | RESULTS AND DISCUSSION

3.1 | Low *OPTN* mRNA level correlates with high stage and poor prognosis of TNBC patients

When we analyzed the correlation between *OPTN* mRNA level and the survival period of TNBC patients, we found that patients with a low *OPTN* level displayed poor prognosis in both relapse-free survival (RFS) (Figure 1A) and distant metastasis-free

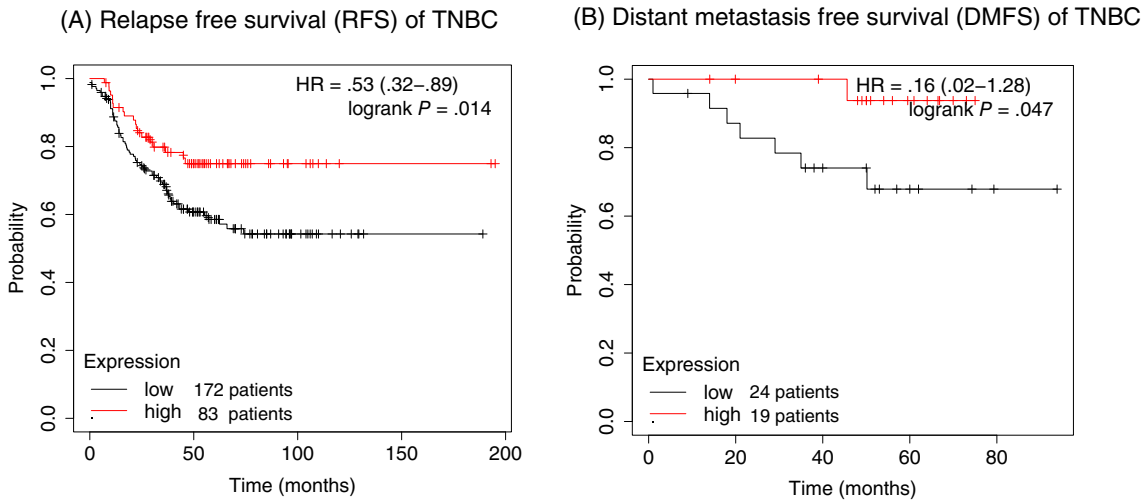

FIGURE 1 Optineurin (OPTN) correlates with better prognosis in triple-negative breast cancer (TNBC) patients. (A) Kaplan-Meier curves (http://kmplot.com/analysis) for the relapse free survival (RFS) of TNBC patients with high and low *OPTN* expression. (B) Kaplan-Meier curves (http://kmplot.com/analysis) for the distant metastasis free survival (DMFS) of TNBC patients with high and low *OPTN* expression.

survival (DFS) (Figure 1B).[24] In addition, we also performed a survival analysis in a TCGA TNBC database and found a similar trend/signature (Figure S1). Taken together, patients with advanced disease and occurrence of metastasis displayed lower *OPTN* mRNA expression level in TNBC. We also performed 5-year survival curves analysis on the whole breast cancer patients including all the subtypes, the analysis showed patients with lower OPTN expression can survive longer (Figure S2). Conversely, TNBC patients with higher OPTN expression can survive longer, which indicates that the favorable role of high OPTN expression relates to TNBC and not when all the breast cancer subtypes are examined together.

3.2 | OPTN suppresses cell migration and extravasation in TNBC zebrafish xenograft model

In order to study the function of OPTN during the TNBC metastasis progress, we generated TNBC MDA-MB-231 OPTN overexpressing cell lines (OPTN-HA & OPTN-FLAG) and knock down cell lines (sh1-OPTN & sh2-OPTN). The misexpression (depletion or ectopic expression) of OPTN was validated by western blot (WB) analysis (Figure 2A,B). Next, we used the scratch assay to dynamically monitor the migration ability of MDA-MB-231 cells with different OPTN expression. The results showed that ectopic OPTN expression in MDA-MB-231 cells migrated slower, while depletion of OPTN in MDA-MB-231 cells increased cell migration (Figure 2C,D). In order to study the OPTN function on TNBC metastasis, we first used a TNBC zebrafish xenograft model by injecting mCherry labeled MDA-MB-231 cells with different OPTN expression levels into the ducts of Cuvier of zebrafish embryos,[21,25] and thereafter analyzed the extravasation ability of different cells in the tail fin (Figure 2E). The results demonstrated that MDA-MB-231 cells with ectopic OPTN expression demonstrated a strong decrease in cell invasion (Figure 2F). Two OPTN knock down cell lines displayed significantly more invasive cells when compared to the empty vector PLKO control cell line (Figure 2G). Consistent with the cell migration results that depletion of OPTN stimulates extravasation, the ectopic expression shows opposite responses. Although ectopic expression (using two independent OPTN expression constructs) is somewhat more prone to artifact than selective genetic knock down, the genetic OPTN depletion (using two independent shRNAs) and its potentiating effect on MDA-MB-231 cell migration and extravasation demonstrate the role of the endogenous protein in this response.

3.3 | OPTN attenuates bone metastasis in TNBC mice xenograft model

To further validate and extend our findings in the zebrafish xenograft TNBC model, we injected intracardially the luciferase labeled bone seeking MDA-MB-231 cells[20] with different OPTN expression levels in the TNBC mice xenograft model, we isolated the metastasis cells from the bones at the endpoint of experiments to analyze the OPTN expression levels and compared those to OPTN levels upon injection (Figure 3A). Consistent with results obtained zebrafish xenograft models, MDA-MB-231 cells with ectopic OPTN expression displayed weaker metastasis spread to the bones as compared to the empty vector control group (Figure 3B,C). The metastasis cells isolated from the bones of different mice showed a decreased OPTN level as compared to the parental cells in both groups. This supports the notion that cells with low OPTN expression exhibit a stronger metastasis ability in the mice xenograft model (Figure 3D). Meanwhile, another parallel mice experiments

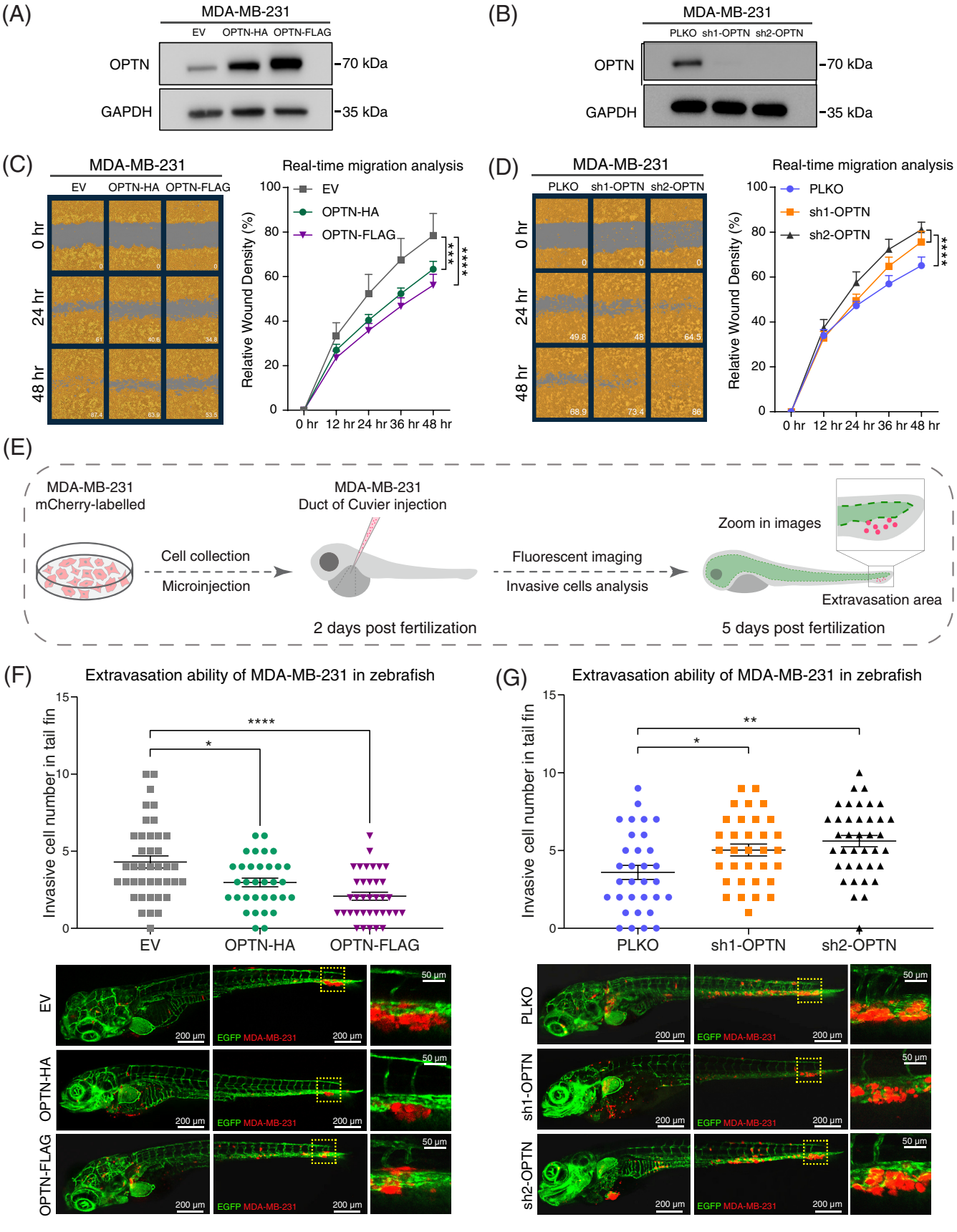

FIGURE 2 Legend on next page.

showed that the most efficient OPTN knock down cell line displayed stronger ability to metastatic size as compared to the PLKO control group (Figure 3E,F). The OPTN levels in the isolated cells from the mice also decreased compared to the parental cells in the PLKO group (Figure 3G). Of note, we found that misexpression of OPTN (by ectopic expression or shRNA-mediated knockdown) does not influence the proliferation characteristics of MDA-MB-231 cells (Figure S3A,B). These findings suggest that that OPTN attenuates metastasis, not proliferation in TNBC xenograft mouse model. While we examined the effect of OPTN misexpression in a bone seeking MDA-MDA-231 clonal variant[20] on bone metastasis, our results cannot rule out (lack of) effects by OPTN of MDA MB 231 cells toward other organs. It will be of interest to repeat OPTN misexpression studies in MDA-MB-231 cells with different tropism to other organs (eg, lung, liver, brain).

3.4 | OPTN inhibits EMT-associated transcription factors and TGFβ signaling transduction in TNBC cells

Most TNBC are basal-like breast cancer, which are mostly characterized by a mesenchymal phenotype and high ability to a metastasize.[26] We next analyzed the effect of OPTN misexpression on the expression level of EMT-associated transcription factors. Our results showed that MDA-MB-231 cells with ectopic OPTN levels displayed decreased protein expression of EMT-associated transcription factors (SNAIL, SLUG and ZEB2) (Figure 4A). In addition, OPTN also inhibited the gene expression of *SNAIL*, *ZEB1* and *ZEB2* in MDA-MB-231 cells (Figure 4B). To validate and obtain further insights into the molecular mechanism, we explored the function of OPTN in controlling TGFβ signal transduction. We found that overexpression of OPTN in MDA-MB-231 cells inhibited TGFβ/SMAD signaling as TGFβ-induced phosphorylation of SMAD2 (a proximal marker for TβRI receptor activity), was decreased. In contrast, knock down of OPTN in MDA-MB-231 cells exhibited an increased TGFβ induced SMAD2 phosphorylation (Figure 4C,D). Similar results were obtained in another TNBC cell line SKBR7 (Figure S4). Furthermore, etopic expression of OPTN also suppressed the TGFβ-induced expression of TGFβ target genes (*PAI-1*, *IL-11* and *PTHrP*) in MDA-MB-231 cells, while genetic depletion of OPTN showed opposite responses (Figure 4E,F). Previous studies showed *IL11* and *PTHrP* are important genes in mediating breast cancer metastasis to bone,[14,27] which is in line with our findings that OPTN suppresses bone metastasis of bone seeking MDA-MB 231 cells in mice xenograft experiments.

3.5 | OPTN regulates TβRI stability by binding and inducing the ubiquitination of TβRI

To uncover how OPTN suppresses TGFβ signaling, we tested the stability of TβRI upon treatment with protein synthesis inhibitor cycloheximide in MDA-MB-231 cells. The results showed that cells with OPTN overexpression induced increased degradation of TβRI (Figure 5A,B), while cells in which OPTN was genetically depleted, demonstrated an increased induced TβRI stability (Figure 5C,D). Next, we examined whether TβRI and OPTN can interact with each other. TβRI and OPTN were found to interact when coexpressed in HEK293T cells, either when TβRI was immunoprecipitated followed by western blotting of OPTN (Figure 5E) or vice versa (Figure 5F). Besides, we found that OPTN binds to the constitutively active (CA) TβRI more avidly than wild type (WT) TβRI (Figure 5G). Importantly, OPTN and TβRI were found to interact with each other at endogenous level in MDA-MB-231 cells, and this interaction can be further increased by TGFβ stimulation (Figure 5H,I). Previous studies have shown that the degradation of TβRI in controlled by polyubiquitination in HEK293T cell.[28,29] We therefore performed the ubiquitination assay of constitutively active mutant of TβRI (caTβRI) in HEK293T cell with or without OPTN knock down. Our results showed that genetic depletion of OPTN can reduce the polyubiquitination of TβRI (Figure 5J). Previous studies showed that K48 polyubiquitination

FIGURE 2 OPTN inhibits MDA-MB-231 cell migration in-vitro and extravasation in-vivo. (A) MDA-MB-231 cell lines with ectopic expression of two OPTN variants (ie, OPTN-HA or OPTN-FLAG) or infected with empty vector (EV) control were established and validated by western blot (WB) analysis. The same blot was used for OPTN and GAPDH (loading control). (B) Two different OPTN shRNA knock down MDA-MB-231 cell lines and control cell line PLKO were established and validated by WB analysis. The same blot was used for OPTN and GAPDH (loading control). (C) Real-time scratch assay results of control and OPTN overexpressing MDA-MB-231 cells. Representative scratch wounds with relative wound density in the right corner are shown at different time point of the experiment (left). The cells are highlighted in orange. Relative wound density (closure) is plotted at indicate times (right). ***P < .001; ****P < .0001; two-way analysis of variance (ANOVA). (D) Real-time scratch assay results of control and OPTN knock down cells. Representative scratch wounds with relative wound density in the right corner are shown at different time point of the experiment (left). The cells are highlighted in orange. Relative wound density (closure) is plotted at indicate times (right). ****P < .0001; two-way analysis of variance (ANOVA). (E), Schematic representation on MDA-MB-231 mCherry-labeled cell injection into zebrafish embryos: collection of cells, microinjection of MDA-MB-231 cells into duct of Cuvier of zebrafish embryos, and analysis of extravasation of MDA-MB-231 cells in the avascular tail fin <5 days post fertilization. (F) Statistics of invasive cell number in tail fin of control and OPTN overexpressing MDA-MB-231 cells in zebrafish xenograft model (above). *P < .05; ****P < .0001; two-way analysis of variance (ANOVA). Representative images of zebrafish from the control and OPTN overexpressing groups with zoom-in of invasive cells on the right panel (below). (G) Statistics of invasive cell number in tail fin of control and OPTN knock down MDA-MB-231 cells in zebrafish xenograft model (above). *P < .05; **P < .01; two-way analysis of variance (ANOVA). Representative images of zebrafish from the control and OPTN knock down groups with zoom-in of invasive cells on the right panel (below).

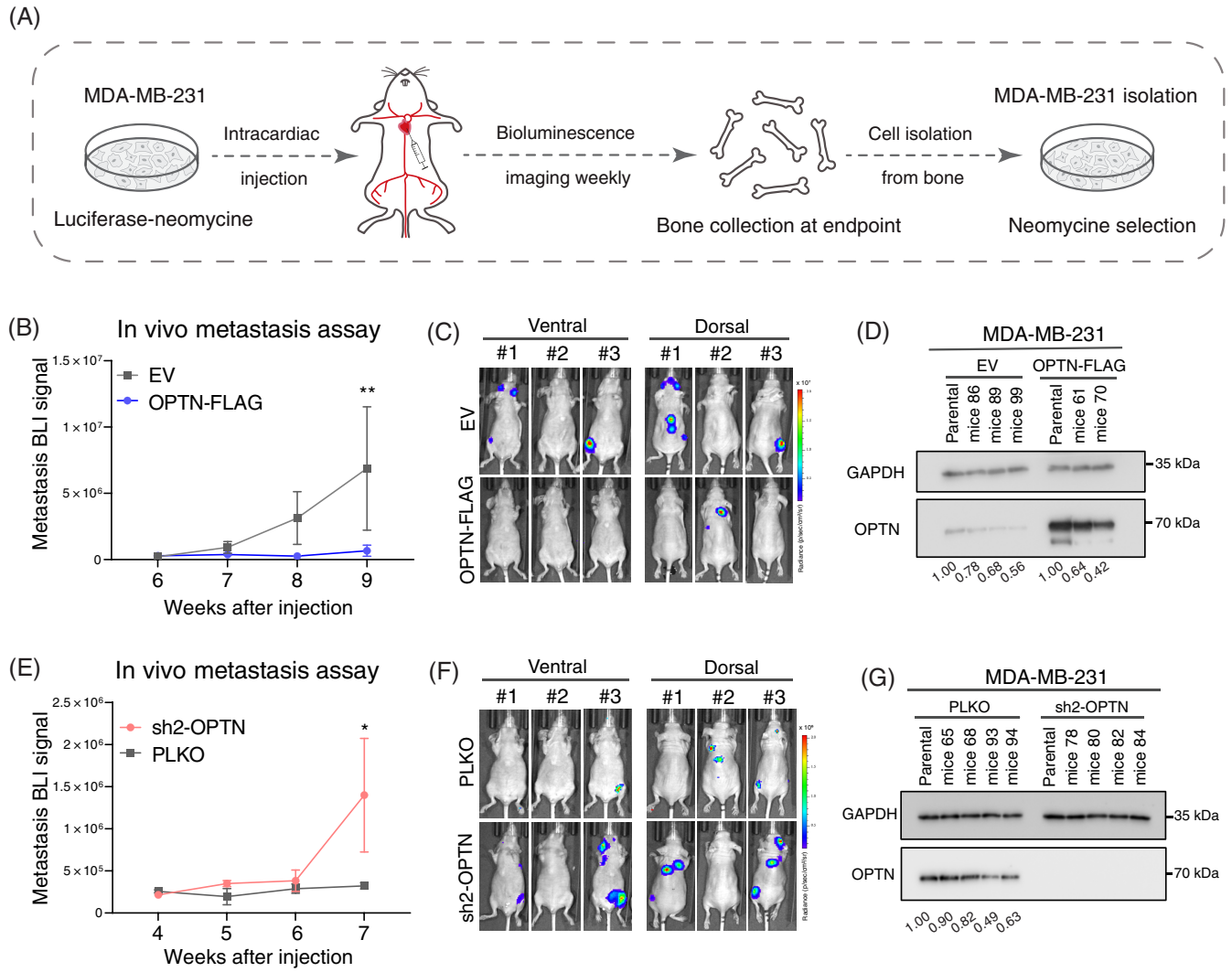

FIGURE 3 OPTN suppresses bone metastasis of MDA-MB-231 cells in vivo. (A) Experimental flow chart of breast cancer bone metastasis assay in mice xenograft model. (B) Bioluminescence imaging (BLI) signal of control and OPTN overexpressing MDA-MB-231 cells were measured at indicated weeks after intracardiac injection. $^{**}P < .01$; two-way ANOVA. (C) Representative images of three mice with BLI signal on both ventral and dorsal side from control and OPTN overexpressing groups at 9 weeks after intracardiac injection. (D) OPTN expression levels were measured by WB analysis of parental cells and metastatic cells isolated from mice bones of control and OPTN overexpressing groups. The same blot was used for OPTN and GAPDH (loading control). OPTN signals were quantified and normalized with GAPDH signals, relative OPTN signal values are indicated below the WB. (E) Bioluminescence imaging (BLI) signals of control and OPTN knock down MDA-MB-231 cells were measured at indicated weeks after intracardiac injection. $^{*}P < .05$; two-way ANOVA. (F) Representative images of three mice with BLI signals on both ventral and dorsal side from control and OPTN knock down groups at 7 weeks after intracardiac injection. (G) OPTN expression levels were measured by WB analysis of parental cells and metastatic cells isolated from mice bones of control and OPTN knock down groups. The same blot was used for OPTN and GAPDH (loading control). OPTN signals were quantified and normalized with GAPDH signals, relative OPTN signal values are indicated below the WB.

was the main ubiquitin chain to regulate TβRI degradation.[30-33] We performed ubiquitin experiments and observed that overexpressing OPTN significantly promoted the K48 ubiquitination of TβRI (Figure 5K). Taken together, our results indicate that OPTN regulates TβRI stability by binding and inducing K48 polyubiquitination of TβRI.

3.6 | *OPTN* mRNA levels negatively correlates with TGFβ response in TNBC patient samples and OPTN inhibits TNBC migration in a TβRI dependent manner

Interrogation of publicly available gene expression databases revealed that a high level of *OPTN* expression correlated with a

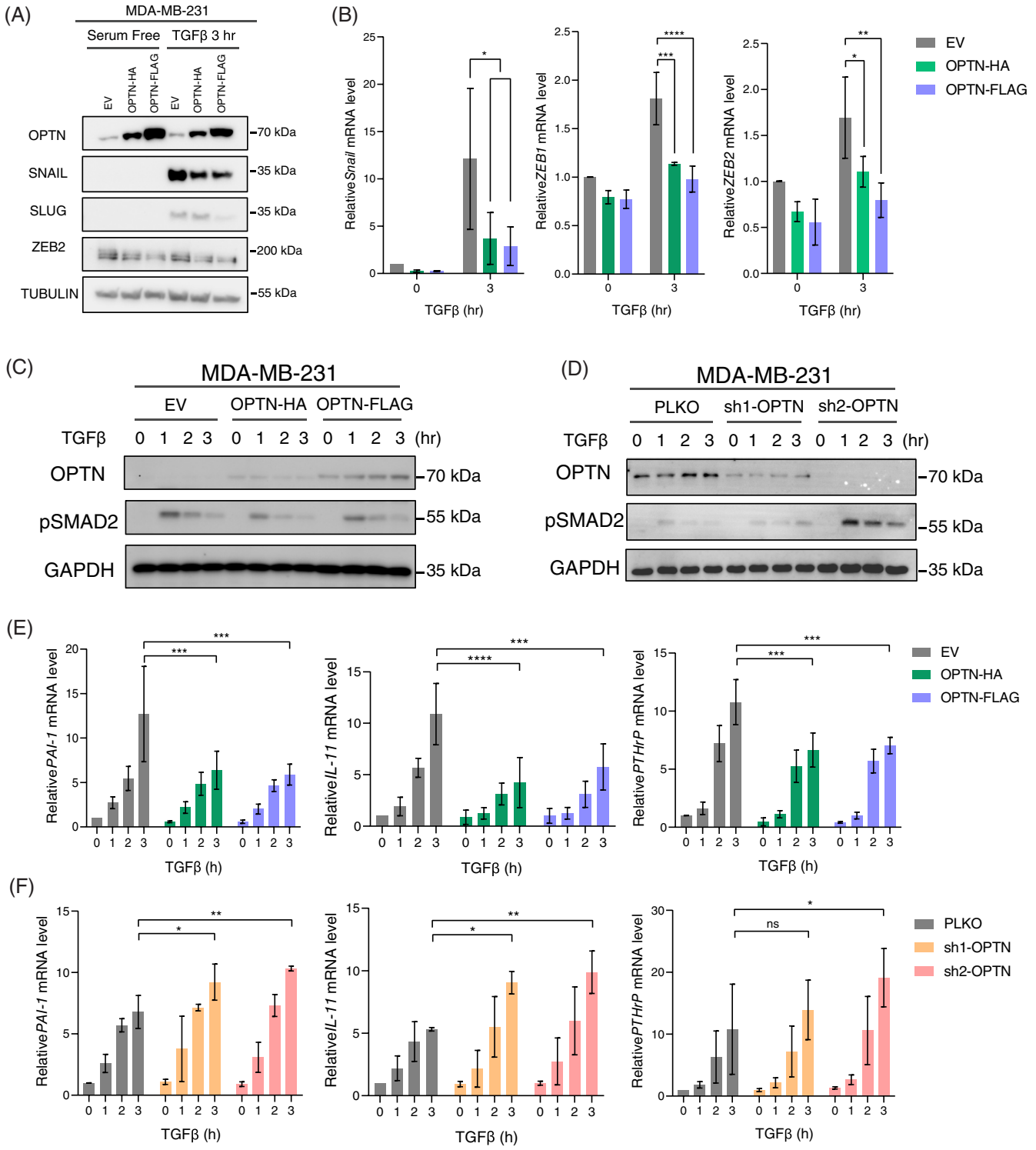

FIGURE 4 OPTN suppresses the expression of mesenchymal markers and inhibits TGFβ signaling transduction in MDA-MB-231 cells. (A) WB analysis of mesenchymal markers in OPTN overexpressing MDA-MB-231 cells. Same blot was used for OPTN, SNAIL and TUBULIN (loading control). ZEB2 and SLUG blotting results were obtained from another blot using the same corresponding cell lysates. (B) Mesenchymal markers including *SNAIL*, *ZEB1* and *ZEB2* were analyzed by qPCR in control and OPTN overexpressing MDA-MB-231 cells. Experiments were performed in triplicate biological repeats; one representative result was shown in the figure. (C) WB analysis of TGFβ-induced pSMAD2 in control and OPTN overexpressing MDA-MB-231 cells. The same blot was used for OPTN, pSMAD2 and GAPDH (loading control). (D) WB analysis of TGFβ-induced pSMAD2 in control and OPTN knock down MDA-MB-231 cells. The same blot was used for OPTN, pSMAD2 and GAPDH (loading control). (E) The TGFβ pathway target genes including *PAI-1*, *IL-11* and *PTHrP* were analyzed by qPCR in control and OPTN overexpressing MDA-MB-231 cells. Experiments were performed in triplicate biological repeats; one representative result was shown in the figure. (F), The TGFβ/SMAD pathway target genes, including *PAI-1*, *IL-11* and *PTHrP*, were analyzed by qPCR in control and OPTN knock down MDA-MB-231 cells. Experiments were performed in triplicate biological repeats; one representative result was shown in the figure.

decreased TGFβ response signature value and low expression of TGFβ target genes *PAI-1* and *CTGF* (Figure 6A). *CTGF* is an important prometastatic TGFβ target gene, which encode osteolytic and angiogenic factors to promote osteolytic metastasis of breast cancer.[14] Thus, *OPTN* RNA expression analysis in TNBC patient derived samples support a suppressor role for OPTN of prometastatic TGFβ signaling. Consistent with this notion, we found that the increased MDA-MB-231 cell migration upon knock down OPTN can be rescued by adding a selective small molecule TβRI kinase inhibitor SB-431542 (SB) (Figure 6B,C). Taken together, our results suggest that OPTN functions as a suppressor of TNBC metastasis (at least in part) through inhibition of the TGFβ prometastatic signaling. Of note, a recent study reported that loss of OPTN triggers immune evasion and

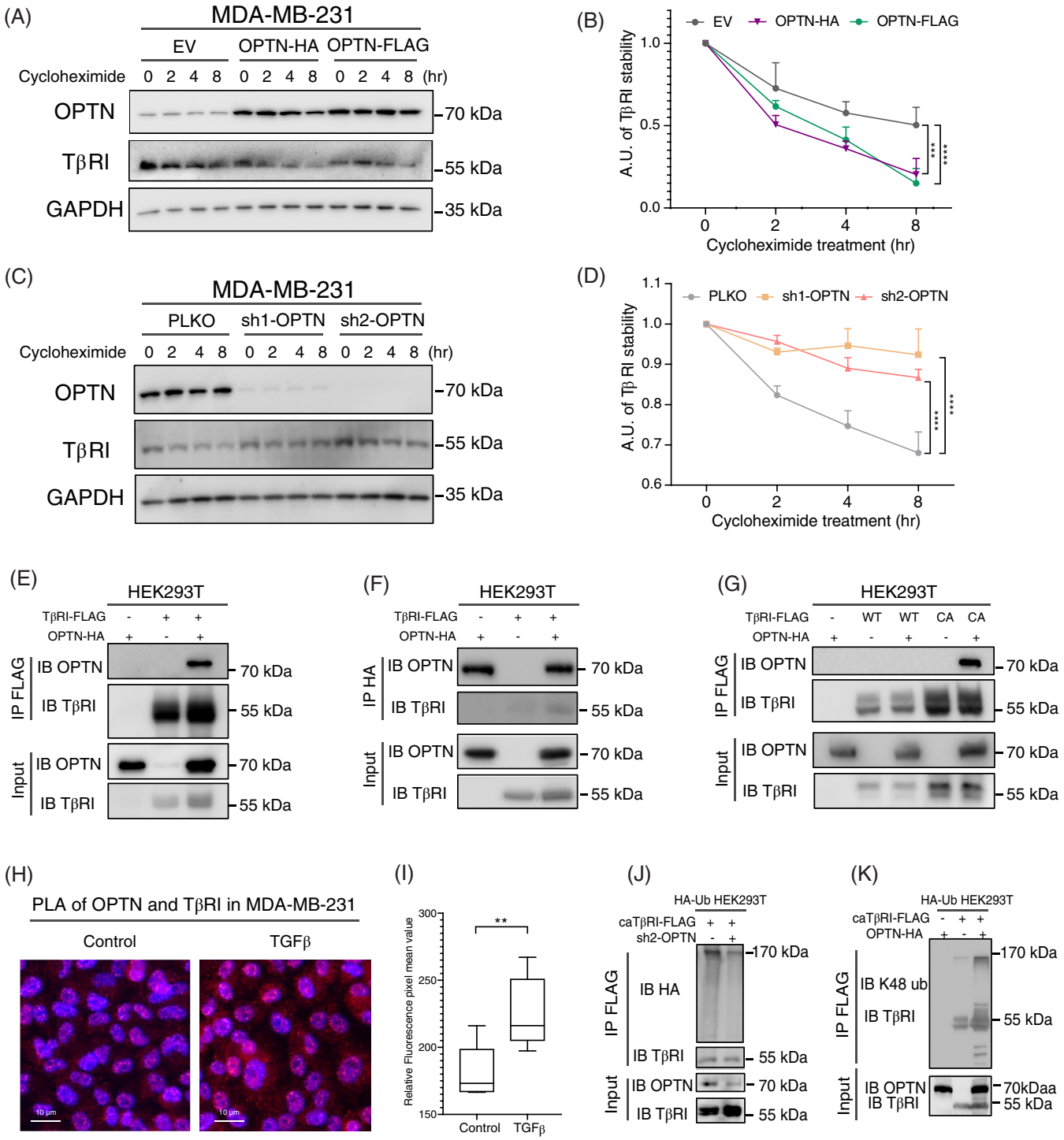

FIGURE 5 Legend on next page.

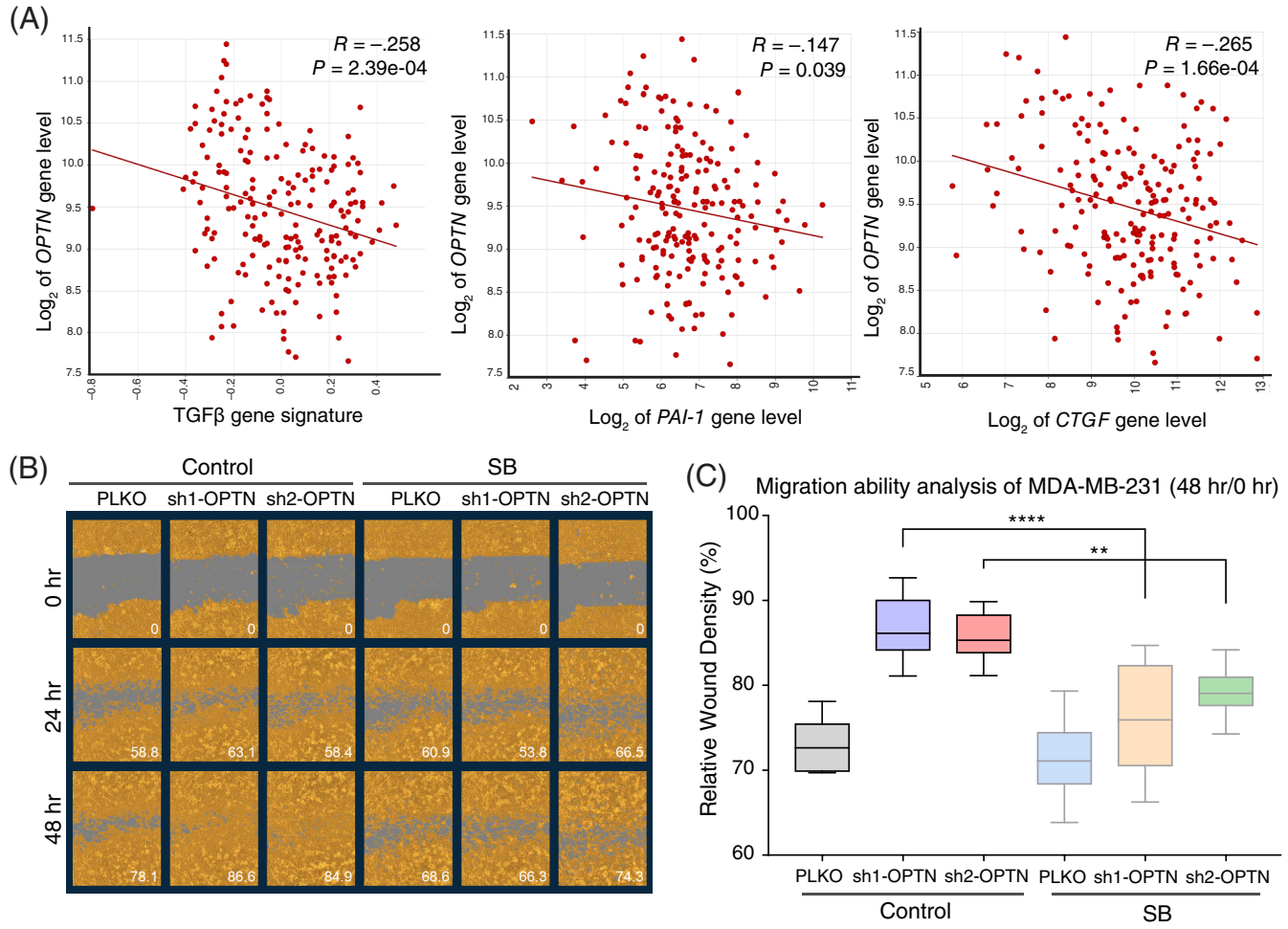

FIGURE 6 Interplay between OPTN and TGFβ/SMAD signaling in TNBC. (A) Correlation analysis between *OPTN* and TGFβ gene signature, *PAI-1* or *CTGF* mRNA expression (two prototypic TGF-β target genes) in TNBC (n = 198). Pearson's correlation coefficient tests were performed to assess the statistical significance. (B) Real-time scratch assays of control and OPTN knock down MDA-MB-231 cells treated with or without TβRI inhibitor SB-431542 (SB). Representative scratch wounds are shown at different time point with relative wound density in the right corner of the experiment. The cells are highlighted in orange. (C) Statistic analysis of migration ability of control and OPTN knock down MDA-MB-231 cells treated with or without SB inhibitor. $^{**}P < .01$; $^{***}P < 0.001$; two-way analysis of variance (ANOVA).

FIGURE 5 OPTN regulates TβRI stability by interacting with TβRI and promoting its K48 polyubiquitination. (A) TβRI stability was analyzed by WB analysis in control and OPTN overexpressing MDA-MB-231 cells treated with 10 μg/mL cycloheximide for different hours. The same blot was used for OPTN, TβRI and GAPDH (loading control). TβRI expression level in control and OPTN overexpressing MDA-MB-231 cells were quantified and statistically analyzed at different time points in (B) $^{***}P < .001$; $^{****}P < .0001$; two-way analysis of variance (ANOVA). (C) TβRI stability was analyzed by WB analysis in control and OPTN knock down MDA-MB-231 cells treated with 10 μg/mL cycloheximide for different hours. The same blot was used for OPTN, TβRI and GAPDH (loading control). TβRI expression level in control and OPTN knock down MDA-MB-231 cells were quantified and statistically analyzed at different time points in (D) $^{****}P < .0001$; two-way analysis of variance (ANOVA). (E) The interaction of OPTN with TβRI was detected by immunoprecipitation (IP) of FLAG-tagged TβRI and immunoblotting (IB) for OPTN in HEK293T cells. (F) The interaction of TβRI with OPTN was detected by immunoprecipitation (IP) of HA-tagged OPTN and IB for TβRI in HEK293T cells. (G) The interactions of wild type (WT) and constitutively active (CA) TβRI with OPTN were analyzed by IP FLAG-tagged TβRI and IB for OPTN in HEK293T cells. IP results were obtained from same blot. Input results were from another blot using the same corresponding cell lysates as used for IP. (H) Proximity ligation assay (PLA) of endogenous interaction of OPTN with TβRI in MDA-MB-231 cells treated with or without 5 ng/mL TGFβ for 1 hour. Lower magnification images are shown in the upper panel; higher magnification images are shown in the lower panel. PLA signals in control and TGFβ treatment groups were quantified and statistically analyzed in (I). $^{**}P < .01$; unpaired Student *t* test. (J) Ubiquitination of TβRI was analyzed by IP of FLAG-tagged constitutively active TβRI (caTβRI) from HA-Ub transfected HEK293T cells with or without OPTN knock down. IP results were obtained from same blot. Input results were obtained from another blot using the same corresponding cell lysates. (K) K48 polyubiquitination of TβRI was detected by IP of FLAG-tagged constitutively active TβRI (caTβRI) from HA-Ub transfected HEK293T cells with or without OPTN overexpression. IP results were obtained from same blot. Input results were obtained from another blot using the same corresponding cell lysates.

immunotherapy resistance in colon cancer.[34] TNBC frequently displays low response to immunotherapy, and high TGFβ signaling activity in cancer cells can mediate immunotherapy resistance.[8] It will therefore be interesting to explore whether TNBC with high OPTN suppresses TNBC metastasis by improving immune response toward TNBC.

4 | CONCLUSION

In the present article, we discovered a role for OPTN in TNBC metastasis. Low *OPTN* mRNA expression levels in TNBC correlated with higher metastasis incidence. Mechanistically, we uncovered that OPTN is a negative regulator of steady levels of TβRI, promoting its K48 ubiquitination and by increasing its turnover. OPTN inhibits TGFβ-induced protumorigenic responses in TNBC cells. Consistently, analysis of TNBC clinical samples revealed that high levels of *OPTN* mRNA levels in TNBC patients correlated with decreased TGFβ gene response signature and decreased expression of TGFβ target genes. Furthermore, the increased migration of TNBC cells by OPTN knockdown was rescued by treatment with a TGFβ receptor kinase inhibitor. Our results identify OPTN expression level as a prognostic indicator for TNBC metastasis.

AUTHOR CONTRIBUTIONS

Conception and design: Sijia Liu and Peter ten Dijke. *Experimentation and acquisition of data*: Sijia Liu and Maarten van Dinther. *Analysis and interpretation of data*: Sijia Liu, Sophie C. Hagenaars, Yuanzhuo Gu, Tom B. Kuipers, Hailiang Mei, Maria Catalina Gomez-Puerto, Wilma E Mesker, Peter ten Dijke. *Writing original daft*: Sijia Liu and Peter ten Dijke. *Editing and revision of manuscript*: All authors. *Technical or material support*: Sophie C. Hagenaars, Wilma E Mesker. *Funding acquisition and project coordination*: Peter ten Dijke. The work reported in the article has been performed by the authors, unless clearly specified in the text.

ACKNOWLEDGEMENTS

Our study was supported by Cancer Genomics Centre Netherlands (CGC-NL) and ZonMW grant (09120012010061). We thank Midory Thorikay for excellent technical assistance, Ronggui Hu (Institute of Biochemistry and Cell Biology, Shanghai Institutes for Biological Sciences, Chinese Academy of Sciences, Shanghai) for OPTN cDNA expression construct, Andrew Hinck (University of Pittsburg, USA) for recombinant TGFβ3 and Martijn Rabelink for providing shRNA lentivirus constructs.

CONFLICT OF INTEREST STATEMENT

The authors declare no conflicts of interest.

DATA AVAILABILITY STATEMENT

The data that support the findings of our study are available at LUMC and can be made available from the corresponding author upon reasonable request.

ETHICS STATEMENT

The study performed with human clinical specimens was approved by the Medical Ethics Committee of the LUMC and was performed in accordance with the Code of Conduct of the Federation of Medical Scientific Societies in the Netherlands (http://www.federa.org/). The studies involving mice models were performed according to standard procedures in compliance with and approved by the Netherlands Cancer Institute Animal Welfare Committee. The zebrafish assays described are not considered animal experiments under the Experiments on Animals Act (Wod, effective 2014), the applicable legislation in the Netherlands in accordance with the European guidelines (EU directive no. 2010/63/EU) regarding the protection of animals used for scientific purposes, because nonself-eating larvae were used. Therefore, a license specific for these assays on zebrafish larvae (<5d) was not required.

ORCID

Sijia Liu https://orcid.org/0000-0002-1326-4932
Maarten van Dinther https://orcid.org/0000-0002-9451-8884
Sophie C. Hagenaars https://orcid.org/0000-0002-9121-1975
Yuanzhuo Gu https://orcid.org/0000-0002-5075-5634
Hailiang Mei https://orcid.org/0000-0003-1781-5508
Maria Catalina Gomez-Puerto https://orcid.org/0000-0002-5362-9780
Wilma E. Mesker https://orcid.org/0000-0001-5533-4778
Peter ten Dijke https://orcid.org/0000-0002-7234-342X

REFERENCES

1. Yin L, Duan JJ, Bian XW, Yu SC. Triple-negative breast cancer molecular subtyping and treatment progress. *Breast Cancer Res*. 2020;22:61. doi:10.1186/s13058-020-01296-5
2. Bianchini G, Balko JM, Mayer IA, Sanders ME, Gianni L. Triple-negative breast cancer: challenges and opportunities of a heterogeneous disease. *Nat Rev Clin Oncol*. 2016;13:674-690. doi:10.1038/nrclinonc.2016.66
3. Al-Mahmood S, Sapiezynski J, Garbuzenko OB, Minko T. Metastatic and triple-negative breast cancer: challenges and treatment options. *Drug Deliv Transl Res*. 2018;8:1483-1507. doi:10.1007/s13346-018-0551-3
4. Mundy GR. Metastasis to bone: causes, consequences and therapeutic opportunities. *Nat Rev Cancer*. 2002;2:584-593. doi:10.1038/nrc867
5. Plunkett TA, Smith P, Rubens RD. Risk of complications from bone metastases in breast cancer. Implications for management. *Eur J Cancer (Oxf, England: 1990)*. 2000;36:476-482. doi:10.1016/s0959-8049(99)00331-7
6. Derynck R, Turley SJ, Akhurst RJ. TGFβ biology in cancer progression and immunotherapy. *Nat Rev Clin Oncol*. 2021;18:9-34. doi:10.1038/s41571-020-0403-1
7. Liu S, Ren J, ten Dijke P. Targeting TGFβ signal transduction for cancer therapy. *Signal Transduct Target Ther*. 2021;6:8. doi:10.1038/s41392-020-00436-9
8. Medina MA, Oza G, Sharma A, et al. Triple-negative breast cancer: a review of conventional and advanced therapeutic strategies. *Int J Environ Res Public Health*. 2020;17:2078. doi:10.3390/ijerph17062078
9. Bhola NE, Balko JM, Dugger TC, et al. TGF-β inhibition enhances chemotherapy action against triple-negative breast cancer. *J Clin Invest*. 2013;123:1348-1358. doi:10.1172/jci65416

10. Colak S, ten Dijke P. Targeting TGF-β signaling in cancer. *Trends Cancer*. 2017;3:56-71. doi:10.1016/j.trecan.2016.11.008
11. Dennler S, Itoh S, Vivien D, ten Dijke P, Huet S, Gauthier JM. Direct binding of Smad3 and Smad4 to critical TGFβ-inducible elements in the promoter of human plasminogen activator inhibitor-type 1 gene. *EMBO J*. 1998;17:3091-3100. doi:10.1093/emboj/17.11.3091
12. Guise TA, Chirgwin JM. Transforming growth factor-β in osteolytic breast cancer bone metastases. *Clin Orthop Relat Res*. 2003;415 Suppl.:S32-S38. doi:10.1097/01.blo.0000093055.96273.69
13. Demirkan B. The roles of epithelial-to-mesenchymal transition (EMT) and mesenchymal-to-epithelial transition (MET) in breast cancer bone metastasis: potential targets for prevention and treatment. *J Clin Med*. 2013;2:264-282. doi:10.3390/jcm2040264
14. Kang Y, Siegel PM, Shu W, et al. A multigenic program mediating breast cancer metastasis to bone. *Cancer Cell*. 2003;3:537-549. doi:10.1016/s1535-6108(03)00132-6
15. Rezaie T, Child A, Hitchings R, et al. Adult-onset primary open-angle glaucoma caused by mutations in optineurin. *Science*. 2002;295:1077-1079.
16. Slowicka K, Vereecke L, van Loo G. Cellular functions of optineurin in health and disease. *Trends Immunol*. 2016;37:621-633. doi:10.1016/j.it.2016.07.002
17. Ying H, Yue BY. Cellular and molecular biology of optineurin. *Int Rev Cell Mol Biol*. 2012;294:223-258. doi:10.1016/b978-0-12-394305-7.00005-7
18. Liu Z, Chen P, Gao H, et al. Ubiquitylation of autophagy receptor optineurin by HACE1 activates selective autophagy for tumor suppression. *Cancer Cell*. 2014;26:106-120.
19. Zhang L, Huang H, Zhou F, et al. RNF12 controls embryonic stem cell fate and morphogenesis in zebrafish embryos by targeting Smad7 for degradation. *Mol Cell*. 2012;46:650-661. doi:10.1016/j.molcel.2012.04.003
20. Deckers M, van Dinther M, Buijs J, et al. The tumor suppressor Smad4 is required for transforming growth factor β-induced epithelial to mesenchymal transition and bone metastasis of breast cancer cells. *Cancer Res*. 2006;66:2202-2209. doi:10.1158/0008-5472.Can-05-3560
21. Ren J, Liu S, Cui C, ten Dijke P. Invasive behavior of human breast cancer cells in embryonic zebrafish. *J Vis Exp*. 2017;122:55459. doi:10.3791/55459
22. Bass JJ, Wilkinson DJ, Rankin D, et al. An overview of technical considerations for Western blotting applications to physiological research. *Scand J Med Sci Sports*. 2017;27:4-25. doi:10.1111/sms.12702
23. Arguello F, Baggs RB, Frantz CN. A murine model of experimental metastasis to bone and bone marrow. *Cancer Res*. 1988;48:6876-6881.
24. Győrffy B, Lanczky A, Eklund AC, et al. An online survival analysis tool to rapidly assess the effect of 22,277 genes on breast cancer prognosis using microarray data of 1,809 patients. *Breast Cancer Res Treat*. 2010;123:725-731. doi:10.1007/s10549-009-0674-9
25. Drabsch Y, He S, Zhang L, Snaar-Jagalska BE, ten Dijke P. Transforming growth factor-β signalling controls human breast cancer metastasis in a zebrafish xenograft model. *Breast Cancer Res*. 2013;15:R106. doi:10.1186/bcr3573
26. Fedele M, Cerchia L, Chiappetta G. The epithelial-to-mesenchymal transition in breast cancer: focus on basal-like carcinomas. *Cancer*. 2017;9:136. doi:10.3390/cancers9100134
27. Yin JJ, Selander K, Chirgwin JM, et al. TGF-β signaling blockade inhibits PTHrP secretion by breast cancer cells and bone metastases development. *J Clin Invest*. 1999;103:197-206. doi:10.1172/jci3523
28. Kavsak P, Rasmussen RK, Causing CG, et al. Smad7 binds to Smurf2 to form an E3 ubiquitin ligase that targets the TGFβ receptor for degradation. *Mol Cell*. 2000;6:1365-1375. doi:10.1016/s1097-2765(00)00134-9
29. Ebisawa T, Fukuchi M, Murakami G, et al. Smurf1 interacts with transforming growth factor-β type I receptor through Smad7 and induces receptor degradation. *J Biol Chem*. 2001;276:12477-12480. doi:10.1074/jbc.C100008200
30. Lönn P, Morén A, Raja E, Dahl M, Moustakas A. Regulating the stability of TGFβ receptors and Smads. *Cell Res*. 2009;19:21-35. doi:10.1038/cr.2008.308
31. Zhang L, Zhou F, Drabsch Y, et al. USP4 is regulated by AKT phosphorylation and directly deubiquitylates TGF-β type I receptor. *Nat Cell Biol*. 2012;14:717-726. doi:10.1038/ncb2522
32. Liu S, González-Prieto R, Zhang M, et al. Deubiquitinase activity profiling identifies UCHL1 as a candidate Oncoprotein that promotes TGFβ-induced breast cancer metastasis. *Clin Cancer Res*. 2020;26:1460-1473. doi:10.1158/1078-0432.ccr-19-1373
33. Kowanetz M, Lönn P, Vanlandewijck M, et al. TGFβ induces SIK to negatively regulate type I receptor kinase signaling. *J Cell Biol*. 2008;182:655-662. doi:10.1083/jcb.200804107
34. Du W, Hua F, Li X, et al. Loss of optineurin drives cancer immune evasion via palmitoylation-dependent IFNGR1 lysosomal sorting and degradation. *Cancer Discov*. 2021;11:1826-1843. doi:10.1158/2159-8290.Cd-20-1571

SUPPORTING INFORMATION

Additional supporting information can be found online in the Supporting Information section at the end of this article.

How to cite this article: Liu S, van Dinther M, Hagenaars SC, et al. Differential optineurin expression controls TGFβ signaling and is a key determinant for metastasis of triple negative breast cancer. *Int J Cancer*. 2023;152(12):2594-2606. doi:10.1002/ijc.34483